

Preferential Latent Space Models for Networks with Textual Edges

Maoyu Zhang¹, Biao Cai², Dong Li³, Xiaoyue Niu⁴, Jingfei Zhang¹

¹ Goizueta Business School, Emory University, Atlanta, GA

² Department of Management Sciences, City University of Hong Kong, Hong Kong, China

³ Department of Statistics and Data Science, Tsinghua University, Beijing, China

⁴ Department of Statistics, Pennsylvania State University, University Park, PA

Abstract

Many real-world networks contain rich textual information in the edges, such as email networks where an edge between two nodes is an email exchange. The useful textual information carried in the edges is often discarded in most network analyses, resulting in an incomplete view of the relationships between nodes. In this work, we represent each text document as a generalized multi-layer network, and introduce a new and flexible preferential latent space network model that can capture how node-layer preferences directly modulate edge probabilities. We establish identifiability conditions for the proposed model and tackle model estimation with a computationally efficient projected gradient descent algorithm. We further derive the non-asymptotic error bound of the estimator from each step of the algorithm. The efficacy of our proposed method is demonstrated through simulations and an analysis of the Enron email network.

Keywords: latent space model; multi-layer network; non-convex optimization; sparsity; text analysis.

1 Introduction

Over the past decades, the study of networks has attracted enormous attention, as they naturally characterize complex systems emerging from many research communities, such as social sciences (Bramoullé et al., 2009; Chen et al., 2022), business (Huang et al., 2020; Gualdani, 2021) and economic research (Pesaran and Yang, 2020; Jin et al., 2024). Many statistical network models have been developed to analyze network data, including the exponential random graph model (Frank and Strauss, 1986; Zhang and Chen, 2015), the stochastic block model (Holland et al., 1983), the random dot product model (Athreya et al., 2018), the network-formation model (Leung, 2015; Bräuning and Koopman, 2020), the latent space model (Hoff et al., 2002; Ma et al., 2020), among others.

The majority of statistical research to date has focused on networks with binary (or weighted) edges that characterize the presence (or strength) of connections between nodes. Meanwhile, networks with textual edges, where an edge between two nodes is a text document, are fast emerging. Examples include email networks, where an edge between two nodes representing email accounts is an email, Twitter networks, where an edge between two nodes representing Twitter accounts is a comment or retweet, and coauthor networks, where an edge between two nodes representing authors is a paper. A common approach to analyze such networks is to discard the textual data and use binary or non-negative integer edges to encode the presence or frequency of exchanges. However, this simplified treatment may lose important information encoded in the text data and offer only an incomplete view of the interactions between nodes in the network. For instance, in email networks, discarding the text data carried in edges can overlook important context information in the email exchanges, and is unable to provide insights on the topics communicated in the emails or the sender/receiver preferences of these topics. To gain a more accurate and com-

prehensive understanding of the relationships between nodes, a more favorable approach is to incorporate the textual information when modeling the formation of network edges.

To extract textual information, useful representation tools from the natural language processing literature can be used. In particular, these tools aim to convert text documents to numerical vectors, which can then be used in text analysis. Some examples include Bag-of-Words that represents tokenized documents as sparse vectors of word counts (Joachims, 1998), sentiment analysis models that convert textual information into sentiment scores (Shapiro et al., 2022), and embedding methods such as Word2Vec (Mikolov et al., 2013), BERT (Devlin et al., 2018), that represent words as dense vectors. These word embedding vectors can capture, for example, semantic similarities and are pre-trained on very large text corpora using neural network models. The appropriate choice of representation tools often depends on the goal of analysis. For example, Word2Vec is useful for learning relationships between words and BERT is useful for translation and next-word prediction (Ke et al., 2023). Dense embedding methods like Word2Vec or BERT may lack interpretability, as it is unclear what each dimension in the embedding space represents, making the vector representations difficult to interpret.

In this paper, we represent each text document between a pair of nodes as a K -variate vector that counts the appearances of K keywords in this document. The K keywords are extracted from all text documents using techniques such as textRank (Mihalcea and Tarau, 2004) or topic modeling (Ke et al., 2023). This text representation approach is a form of Bag-of-Words where the dictionary is refined to be keywords in the corpus, and it greatly facilitates model interpretability. Effectively, we convert a text document between nodes i, j to a multivariate edge of dimension K , denoted as $y_{ijl} = (y_{ijl}^{(1)}, \dots, y_{ijl}^{(K)})$, where $y_{ijl}^{(k)}$ counts the appearance of keyword k in document l between nodes i, j . In this paper,

we refer to the network with edges y_{ijl} 's as a *generalized multi-layer network*, where each edge dimension is referred to as a *layer*. Unlike a typical multi-layer network, a unique aspect of our data is that the number of nonzero multivariate edges between nodes can vary. For example, nodes i, j may exchange 2 emails, while nodes i', j' exchange 20. As such, if each email is treated as a separate observation of edges between nodes, our data cannot be conveniently structured into a typical multi-layer network, where no more than one nonzero edge exists between a pair of nodes.

To model this generalized multi-layer network, we propose a new preferential latent space framework that models edge probabilities as a function of latent node positions and node-layer preferences represented via parameter $W \in \mathbb{R}^{n \times K}$, where n is the number of nodes in the network and W_{ik} characterizes the interest level of node i on layer k . The weight (W_{ik}, W_{jk}) varies across node pairs and layers, allowing the model to flexibly account for varying interest levels from nodes on layers and give direct insights on how contents of the textual exchanges modulate the relationships between nodes. As the number of keywords K can be large, we further impose a sparsity assumption on W to improve model estimability and interpretability. We tackle model estimation with a computationally efficient projected gradient descent algorithm and theoretically derive the error bound of the estimator from each step of the algorithm. Our newly proposed preferential latent space model is general and can be used to model other multi-layer networks, particularly when there are heterogeneous node-layer preferences. Examples include multi-layer social networks, where users interact on different platforms, such as Facebook, Twitter, Instagram, with varying levels of engagement, and international trade networks, where countries trade on different products with varying levels of demands.

Our work contributes to both methodology and theory. As to methodology, we pro-

pose a flexible preferential latent space model for generalized multi-layer networks. The proposed model is able to effectively borrow information across a large number of sparse layers when estimating the latent node positions and also provide direct insights into the heterogeneous node-layer preferences. With respect to theory, we establish an explicit error bound for the projected gradient descent iterations that shows an interesting interplay between computational and statistical errors. Specifically, it demonstrates that as the number of iterations increases, the computational error of the estimates converges geometrically to a neighborhood that is within statistical precision of the unknown true parameter. The theoretical analysis is nontrivial, as it involves alternating gradient descent, orthogonal transformation, identifiability constraints, sparsity, and the non-quadratic form of the loss function.

Some recent works considered modeling networks with edges that contain textual information. For example, [Sachan et al. \(2012\)](#); [Bouveyron et al. \(2018\)](#); [Corneli et al. \(2019\)](#); [Boutin et al. \(2023\)](#) considered Bayesian community-topic models that extended the latent Dirichlet allocation model to incorporate network communities. These works assume nodes in the network form several communities and the focus is to identify the community label of each node. Model estimation in these works is often carried out via Gibbs sampling or variational EM, which may be prohibitive when applied to large networks. In comparison, our goal is to understand the relationships between nodes and we do not impose assumptions on the community structure amongst nodes. There is another closely related line of research on modeling standard multi-layer networks, which are special cases of the generalized multi-layer networks we study, by allowing only one nonzero multivariate edge between two nodes. From our data, standard multi-layer networks can be constructed by merging the text documents between a pair of nodes into one. In this case, the edge between nodes

i, j on layer k counts the appearance of keyword k in all of the text documents between nodes i, j . For multi-layer networks, [Paul and Chen \(2020\)](#); [Lei et al. \(2020\)](#); [Jing et al. \(2021\)](#); [Agudze et al. \(2022\)](#); [Lei and Lin \(2023\)](#); [Lyu et al. \(2023\)](#) and others considered community detection, and [Gollini and Murphy \(2016\)](#); [Salter-Townshend and McCormick \(2017\)](#); [D’Angelo et al. \(2019\)](#) studied Bayesian latent space models. Recently, [Zhang et al. \(2020\)](#); [Arroyo et al. \(2021\)](#) considered multi-layer network models that assume common latent node positions and layer-specific scaling matrices. However, the layer-specific scaling matrix scales all latent node positions equally and is unable to capture the varying level of interests from nodes on a specific layer. [Wang et al. \(2023\)](#) introduced multi-layer random dot product graph model and developed a novel nonparametric change point detection algorithm. [MacDonald et al. \(2022\)](#) proposed a novel latent space model where the latent node positions are concatenations of common position coordinates and layer-specific position coordinates. This model may not work well when there is a large number of sparse layers, as it is challenging to estimate the layer-specific positions in this case. We compare with both [Zhang et al. \(2020\)](#) and [MacDonald et al. \(2022\)](#) in simulations and real data analysis. In particular, we find that our proposed method enjoys better prediction accuracy in the analysis of a real email network.

The rest of our paper is organized as follows. Section 2 introduces the preferential latent space model for networks with multivariate edges and Section 3 discusses model estimation. Section 4 investigates theoretical properties of the estimator from our proposed algorithm. Section 5 reports the simulation results, and Section 6 conducts an analysis of the Enron email corpus data. The paper is concluded with a short discussion section.

2 Preferential Latent Space Model

We start with some notation. Let $[k] = \{1, 2, \dots, k\}$. Given a vector $x \in \mathbb{R}^d$, we use $\|x\|_0$, $\|x\|_2$ and $\|x\|_\infty$ to denote the vector ℓ_0 , ℓ_2 and ℓ_∞ norms, respectively. Write $\langle a, b \rangle = \sum_i a_i b_i$ for $a, b \in \mathbb{R}^n$. For a matrix $X \in \mathbb{R}^{d_1 \times d_2}$, let $\|X\|_F$ and $\|X\|_{op}$ denote the Frobenius norm and operator norm of X , respectively, and $\|X\|_0 = \sum_{ij} 1(X_{ij} \neq 0)$ denote the number of nonzero entries. We use $\text{Diag}(x_1, \dots, x_d)$ to denote a $d \times d$ diagonal matrix with diagonal elements x_1, \dots, x_d , and use \circ to denote the Hadamard product. For two positive sequences a_n and b_n , write $a_n \lesssim b_n$ or $a_n = O(b_n)$ if there exist $c > 0$ and $N > 0$ such that $a_n < cb_n$ for all $n > N$, and $a_n = o(b_n)$ if $a_n/b_n \rightarrow 0$ as $n \rightarrow \infty$; write $a_n \asymp b_n$ if $a_n \lesssim b_n$ and $b_n \lesssim a_n$.

Suppose there are n nodes in the network, and between nodes i, j , there are m_{ij} document exchanges denoted as $\{z_{ijl}\}_{l \in [m_{ij}]}$. Each z_{ijl} is a tokenized document consisting of a list of words. From the corpus $\{z_{ijl}\}_{i, j \in [n], l \in [m_{ij}]}$, we extract a set of K keywords. These keywords can be defined as words with high co-occurrence frequencies with other words in the corpus, using the textRank algorithm (Mihalcea and Tarau, 2004), or as words that represent latent topics within the corpus, using topic modeling techniques (Ke et al., 2023). Correspondingly, each document z_{ijl} can be represented as a K -dimensional vector $y_{ijl} = (y_{ijl}^{(1)}, \dots, y_{ijl}^{(K)})$, where $y_{ijl}^{(k)}$ characterizes the appearance of keyword k in document z_{ijl} . In this work, we refer to $y_{ijl}^{(k)}$ as an edge when there is no ambiguity and y_{ijl} as a multivariate edge. To ease exposition, we focus on undirected binary-valued edges, that is, $y_{ijl}^{(k)} = y_{jil}^{(k)} \in [0, 1]$, although our methods and results generalize directly to directed edges and other types of edge values, such as continuous and non-negative integers, using tools in generalized linear models. In summary, the network data we model can be denoted as $Y = \{Y_{ij}\}_{i, j \in [n]}$, where $Y_{ij} \in [0, 1]^{m_{ij} \times K}$ collects the m_{ij} multivariate edges between nodes (i, j) , and the l th row of Y_{ij} is the length- K vector, y_{ijl} . If there is no exchange between

nodes i and j , we define $Y_{ij} = (0, \dots, 0) \in [0, 1]^K$.

We adopt a conditional independence approach (Hoff et al., 2002) which assumes each node i has a unique latent position $u_i \in \mathbb{R}^d$. Letting $U = [u_1, \dots, u_n]^\top$, the model admits

$$\text{pr}(Y | U, \theta) = \prod_{i \neq j, l, k} \text{pr}(y_{ijl}^{(k)} | u_i, u_j, \theta),$$

where θ collects other model parameters to be estimated. Given U and θ , we assume that $y_{ijl}^{(k)}$ follows a Bernoulli distribution, with $\Theta_{ij}^{(k)} = \log \text{odds}(y_{ijl}^{(k)} = 1 | U, \theta)$ and

$$\Theta_{ij}^{(k)} = a_i + a_j + (W_{ik}u_i^\top)(W_{jk}u_j), \quad (1)$$

where $a_i \in \mathbb{R}$ represents the node-specific baseline effect and $W_{ik} \geq 0$ is a weight parameter that quantifies the interest level of node i in layer k . In particular, a larger W_{ik} indicates a greater interest of node i in layer k . If either node i or j is uninterested in layer k , meaning $W_{ik} = 0$ or $W_{jk} = 0$, then the log odds of $y_{ijl}^{(k)} = 1$ reduces to the baseline level $a_i + a_j$. The parameters u_i and u_j are latent node positions, and the angle between them determines the likelihood of edges between nodes i and j . When u_i and u_j point in the same direction, that is, $u_i^\top u_j > 0$, the two nodes are more likely to have an edge in any layer k . Additionally, if both nodes i and j have strong interests in layer k , meaning large W_{ik} and W_{jk} , the likelihood of an edge between nodes i and j in layer k is further increased. See Figure 1 for an illustration.

We refer to model (1) as the *preferential latent space model* (PLSM) and discuss model identifiability conditions at the end of this section. In this model, the probability of an edge between nodes i, j in layer k is determined by $W_{ik}W_{jk}u_i^\top u_j$. The multiplied weight $W_{ik}W_{jk}$ varies across node pairs and layers, allowing the model to flexibly account for varying inter-

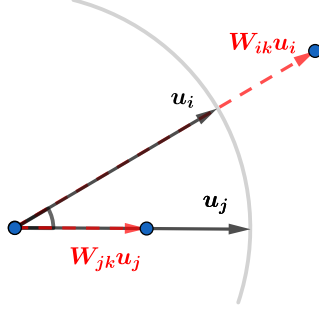


Figure 1: An illustration of the preferential latent space model.

est levels from nodes on layers. From this perspective, the proposed model is more flexible than Zhang et al. (2020); Arroyo et al. (2021). The baseline effect $a = (a_1, \dots, a_n)^\top$ and latent positions in U are shared across all layers, enabling model (1) to borrow information across a large number of sparse layers when estimating these parameters. When K is large, we impose element-wise sparsity on W to ensure its estimability. This stipulates that each node prefers only a subset of the K layers, or equivalently, each layer is only preferred by only a subset of the nodes. This plausible assumption effectively reduces the number of parameters while enhancing model interpretability.

The following proposition states a sufficient condition for the identifiability of model (1), and its proof is collected in the supplement.

Proposition 1 (Identifiability) *Suppose two sets of parameters (a, W, U) and $(a^\dagger, W^\dagger, U^\dagger)$ satisfy the following conditions:*

- (1) $\|u_i\|_2 = 1, \|u_i^\dagger\|_2 = 1$ for $i \in [n]$.
- (2) $W_{i'k'} = 0, W_{i'k'}^\dagger = 0$ for some $i' \in [n], k' \in [K]$.

Then, if the following holds for $i, j \in [n], k \in [K]$,

$$a_i + a_j + (W_{ik}u_i^\top)(W_{jk}u_j) = a_i^\dagger + a_j^\dagger + (W_{ik}^\dagger u_i^{\dagger\top})(W_{jk}^\dagger u_j^\dagger),$$

there exists an orthonormal matrix $R \in \mathbb{R}^{d \times d}$ satisfying $R^\top R = RR^\top = I_d$, such that $a^\dagger = a$, $W^\dagger = W$ and $U^\dagger = UR$.

Condition (1) in the above proposition is a norm constraint, imposed to ensure W and U are identifiable. This condition confines all latent node positions to the unit sphere. Condition (2) assumes at least one entry in W is zero and this is imposed to ensure W and a are identifiable.

3 Estimation

Given network data $Y = \{Y_{ij}\}_{i,j \in [n]}$, where $Y_{ij} \in [0, 1]^{m_{ij} \times K}$, we aim to estimate a , W , and U . Under model (1), the negative log-likelihood function, up to a constant, can be written as

$$\ell(a, W, U) = - \sum_{k=1}^K \sum_{i < j}^n \sum_{l=1}^{m_{ij}} \frac{1}{m_{ij}} \left\{ y_{ijl}^{(k)} \Theta_{ij}^{(k)} + \log \left(1 - \psi(\Theta_{ij}^{(k)}) \right) \right\}, \quad (2)$$

where $\psi(x) = 1/(1 + \exp(-x))$. We consider the following optimization problem,

$$\min_{a \in \mathbb{R}^n, W \in \mathbb{R}_+^{n \times K}, U \in \mathbb{R}^{n \times d}} \ell(a, W, U), \quad \text{subject to } \|W\|_0 \leq s, \quad (3)$$

where s is a tuning parameter that controls the sparsity of W . To enforce sparsity and the positivity constraint on W along the solution path, we employ a truncation operator $\text{Truncate}(W, s)$ for $s \leq nK$ such that $[\text{Truncate}(W, s)]_{ik} = W_{ik}$ if $(i, k) \in \text{Supp}^+(W, s)$ and $[\text{Truncate}(W, s)]_{ik} = 0$ otherwise, where $\text{Supp}^+(W, s)$ denotes the s entries in W with the largest values. To solve (3), we develop a projected gradient descent algorithm that is easy to implement and computationally efficient. Our estimation procedure is summarized in Algorithm 1.

The parameters η_a, η_W, η_U control the step sizes in the gradient descent algorithm.

Algorithm 1 Projected Gradient Descent Algorithm

Input: network data Y , initial values $a^{(0)}, \mathbf{W}^{(0)}, U^{(0)}$, step sizes η_a, η_W, η_U .

repeat for $t = 0, 1, \dots$,

$$a^{(t+1)} = a^{(t)} - \eta_a \nabla_a \ell(a, W^{(t)}, U^{(t)})|_{a=a^{(t)}};$$

$$W^{(t+1)} = \text{Truncate}(W^{(t)} - \eta_W \nabla_W \ell(a^{(t)}, W, U^{(t)})|_{W=W^{(t)}, s});$$

$$U^{(t+1)} = U^{(t)} - \eta_U \nabla_U \ell(a^{(t)}, W^{(t)}, U)|_{U=U^{(t)}}; \text{ normalize rows of } U^{(t+1)};$$

until the objective function converges.

Output a, W , and U

Theorem 1 provides theoretical conditions on η_a, η_W, η_U to ensure the algorithm achieves a linear convergence rate. In practice, backtracking line search can be implemented for η_a, η_W, η_U at each step of the iteration to achieve fast convergence.

For the initialization of Algorithm 1, we consider a singular value thresholding based approach (Ma et al., 2020), which has demonstrated good empirical performance. See Section S1 in the supplement for details. The latent dimension d and the sparsity s are two tuning parameters in the proposed model. We select these two parameters using edge cross-validation (Li et al., 2020). Specifically, we divide all indices $\{i, j, l, k\}$'s into L folds and use each fold as a validation set while training the model on the remaining $L - 1$ folds. To calculate the cross-validation error on the validation set, we calculate the binomial deviance, and the d and s combination with the smallest cross-validation error is selected.

4 Theoretical Results

We define the parameter space as

$$\mathcal{F}_{n,d,K}(M_1) = \left\{ (a, W, U) \mid \|a\|_\infty \leq M_1/4, \max_i \sum_{k=1}^K (W_{ik})^2 \leq M_1/2, \|W\|_0 < nK, \right. \\ \left. \|u_i\|_2 = 1, \max_{i \neq j,k} \Theta_{ij}^{(k)} \leq -(1-C)M_1 \right\}, \quad (4)$$

where $M_1 \geq 0$ is a scalar that may depend on n and $0 < C < 1$ is a constant. By the definition of $\Theta_{ij}^{(k)}$ in (1) and combining $\|a\|_\infty \leq M_1/4$, $\max_i \sum_{k=1}^K (W_{ik})^2 \leq M_1/2$ and $\|u_i\|_2 = 1$ in (4), it is straightforward to show that $\max_{i,j,k} |\Theta_{ij}^{(k)}| \leq M_1$. Hence, for any $(a, W, U) \in \mathcal{F}_{n,d,K}(M_1)$, $\Theta_{ij}^{(k)}$'s are uniformly bounded in $[-M_1, -(1-C)M_1]$ for any k and $i \neq j$. That is, edge probabilities $\psi(\Theta_{ij}^{(k)})$'s are bounded between $1/(1+e^{M_1})$ and $1/(1+e^{(1-C)M_1})$. It is seen that M_1 controls the overall sparsity of the network. If, for example, M_1 is in the order of $\log(n) - \log \log(n)$, then the average edge probability is in the order of $\log(n)/n$.

Let (a^*, W^*, U^*) be the true parameter, $\sigma_1^* \geq \dots \geq \sigma_d^* > 0$ be the nonzero singular values of U^* and $s^* = \|W^*\|_0$. Write $w_{\max} = \max_k w_{\max}^{(k)}$, where $w_{\max}^{(k)} = \max_i W_{ik}^*$ is the maximum entry in column $W_{.k}^*$, and $w_{\min} = \min_k w_{\min}^{(k)}$, where $w_{\min}^{(k)} = \min_{i:W_{ik}^* \neq 0} W_{ik}^*$ is the minimum nonzero entry in column $W_{.k}^*$. We assume $w_{\max} \asymp w_{\max}^{(k)}$ and $w_{\min} \asymp w_{\min}^{(k)}$ for any k . This assumption is made to simplify notations in our analysis, and our results hold under more general conditions on W_{ik}^* 's but with more involved notations. We denote $\bar{m} = (\max_i 1/n \sum_j 1/m_{ij})^{-1}$, where \bar{m} characterizes the average number of edges. To further simplify notation, we assume $\min_{ij} m_{ij} = O(1)$, that is, the minimum number of edges between two nodes is a constant.

We first introduce an error metric for the iterates from Algorithm 1. As U is identifiable up to an orthogonal transformation, for any $U_1, U_2 \in \mathbb{R}^{n \times d}$, we define a distance measure

$$\text{dist}(U_1, U_2) = \min_{R: RR^\top = I} \|U_1 - U_2 R\|_F.$$

Next, we define the error from step t in Algorithm 1 as

$$e_t = 2Kn \|a^{(t)} - a^*\|_2^2 + \sigma_1^{*2} w_{\max}^2 \|W^{(t)} - W^*\|_F^2 + K\sigma_1^{*2} w_{\max}^4 \text{dist}^2(U^{(t)}, U^*). \quad (5)$$

We first derive an error bound for e_t in Theorem 1, and then derive error bounds for $a^{(t)}$, $W^{(t)}$ and $U^{(t)}$, respectively, in Corollary 1. We assume the following regularity conditions.

Assumption 1 Let $\kappa_0 = (\sigma_1^* w_{\max}^2)/(\sigma_d^* w_{\min}^2)$. Assume initial values $a^{(0)}$, $W^{(0)}$ and $U^{(0)}$ satisfy

$$e_0 \leq C_1 K \sigma_1^{*4} w_{\max}^4 \kappa_0^{-4} e^{-2M_1},$$

for a sufficiently small constant $C_1 > 0$.

This assumption requires the initial values to be reasonably close to the true parameters. Such assumptions are commonly employed in nonconvex optimizations (Lyu et al., 2023; Zhang et al., 2023). In particular, if $\kappa_0 = O(1)$ and $d = O(1)$, then Assumption 1 can be simplified to $\|a^{(0)} - a^*\|_2^2 = O(nw_{\max}^4 e^{-2M_1})$, $\|W^{(0)} - W^*\|_F^2 = O(Knw_{\max}^2 e^{-2M_1})$ and $\text{dist}^2(U^{(0)}, U^*) = O(ne^{-2M_1})$. These assumptions on $a^{(0)}$, $W^{(0)}$ and $U^{(0)}$ are relatively mild.

Assumption 2 Assume the following holds for a sufficiently large constant $C_2 > 0$,

$$K\sigma_d^{*2} \geq C_2(w_{\max}^2/w_{\min}^4) \max\{n/\bar{m}, \log(n)\} e^{CM_1}.$$

This is an assumption on the minimal signal strength σ_d^* , which is the minimum nonzero singular value of U^* . It is seen that the signal strength condition weakens as the number of layers K or average number of edges \bar{m} increases. Also, the signal strength condition becomes stronger as M_1 increases, corresponding to sparser networks.

Theorem 1 Suppose $(a^{(0)}, W^{(0)}, U^{(0)})$ satisfies Assumption 1 and (a^*, W^*, U^*) is in (4) and satisfies Assumption 2. Letting $\eta_a = \eta/(4Kn)$, $\eta_W = \eta/(4\sigma_1^{*2}w_{\max}^2)$, $\eta_U = \eta/(2K\sigma_1^{*2}w_{\max}^4)$ and $s = \gamma s^*$ for $\gamma > 1$, the t -th step iteration of Algorithm 1 satisfies, with probability as

least $1 - Kn^{-1}$,

$$e_t \lesssim \rho^t e_0 + \kappa_0^4 e^{(1+C)M_1} [d \max \{n/\bar{m}, \log(n)\} + s^* \log(n)/\bar{m}],$$

where $0 < \rho < 1/2$ and $\eta = \kappa_0^2(16 - \rho)e^{M_1}/4$.

This theorem describes the estimation error at each iteration and provides theoretical guidance on step sizes η_a , η_W and η_U in Algorithm 1. The error bound consists of two terms. The first term $\rho^t e_0$ is the computational error, which decays geometrically with the iteration number t since the contraction parameter ρ satisfies $0 < \rho < 1/2$. The second term $\kappa_0^4 e^{(1+C)M_1} [d \max \{n/\bar{m}, \log(n)\} + s^* \log(n)/\bar{m}]$ represents the statistical error, which is related to noise in the data and does not vary with t . These two terms reveal an interesting interplay between the computational efficiency and statistical rate of convergence. Specifically, when the number of iterations is sufficiently large, the computational error is to be dominated by the statistical error and the resulting estimator falls within the statistical precision of the true parameters. In the statistical error, the term $s^* \log(n)/\bar{m}$ is related to estimating the sparse matrix W^* and the term $d \max \{n/\bar{m}, \log(n)\}$ is related to estimating the low-rank matrix U^* . The statistical error decreases with the average number of edges \bar{m} and increases with the sparsity parameter M_1 .

Our theoretical analysis is nontrivial as the node-layer preferential effects in $W_{ik}W_{jk}u_i u_j$ lead to an involved interplay between W and U . This requires carefully bounding the error of $W^{(t)}$ and $U^{(t)}$ (up to rotation) in each step of the iteration to achieve contraction while ensuring the identifiability conditions are met. To tackle varying edge number m_{ij} 's, we derive a tight bound on the spectrum of random matrices with bounded moments following the techniques in [Bandeira and van Handel \(2016\)](#); see Lemma S5. This bound is sharper than the matrix Bernstein inequality ([Tropp, 2012](#)). Using Lemma S5, we are able to improve

the statistical error for low rank matrix U^* from $\kappa_0^4 e^{(1+C)M_1} dn \log(n)$, which can be derived using the matrix Bernstein inequality under $m_{ij} = 1$, to $\kappa_0^4 e^{(1+C)M_1} d \max\{n/\bar{m}, \log(n)\}$, which in turn relaxes the minimal signal strength condition in Assumption 2.

Corollary 1 *Under the same conditions in Theorem 1, for any*

$t \geq \log \left[\{d \max\{n/\bar{m}, \log(n)\} + s^* \log(n)/\bar{m}\} \kappa_0^8 e^{(3+C)M_1} / (C_1 K \sigma_1^{*4} w_{\max}^4) \right] / \log(\rho)$, *it holds*

that

$$\begin{aligned} \|a^{(t)} - a^*\|_2^2 &\lesssim \frac{\kappa_0^4 e^{(1+C)M_1}}{K} \left[d \max \left\{ \frac{1}{\bar{m}}, \frac{\log(n)}{n} \right\} + \frac{s^* \log(n)}{n\bar{m}} \right], \\ \|W^{(t)} - W^*\|_F^2 &\lesssim \frac{\kappa_0^4 e^{(1+C)M_1}}{w_{\max}^2} \left[d \max \left\{ \frac{1}{\bar{m}}, \frac{\log(n)}{n} \right\} + \frac{s^* \log(n)}{n\bar{m}} \right], \\ \text{dist}^2(U^{(t)}, U^*) &\lesssim \frac{\kappa_0^4 e^{(1+C)M_1}}{K w_{\max}^4} \left[d \max \left\{ \frac{1}{\bar{m}}, \frac{\log(n)}{n} \right\} + \frac{s^* \log(n)}{n\bar{m}} \right], \end{aligned}$$

with probability at least $1 - Kn^{-1}$.

In Corollary 1, the error bounds for $a^{(t)}$ and $U^{(t)}$ decrease with K , indicating that their estimation improves as the number of layers K increases. All three estimation errors decrease with the average number of edges \bar{m} , suggesting that observing more edges between nodes leads to better estimation. Finally, the estimation error for U^* matches with that in standard latent space models (Ma et al., 2020) when $K = 1$, $\bar{m} = 1$ and $W_{ij} = 1$ for all i, j .

5 Simulation

In this section, we evaluate the finite sample performance of our proposed method. We also compare with some alternative solutions, and the results are collected in the supplement. Specifically, we investigate how estimation and variable selection accuracy in simulations vary with network size n , the number of layers K , edge density and the number of edges m_{ij} between nodes. We simulate data from model (1) with parameters a^* , W^* and U^* . For a^* , we generate its entries independently from $\text{Uniform}(a_l, a_u)$, where a_l and a_u together

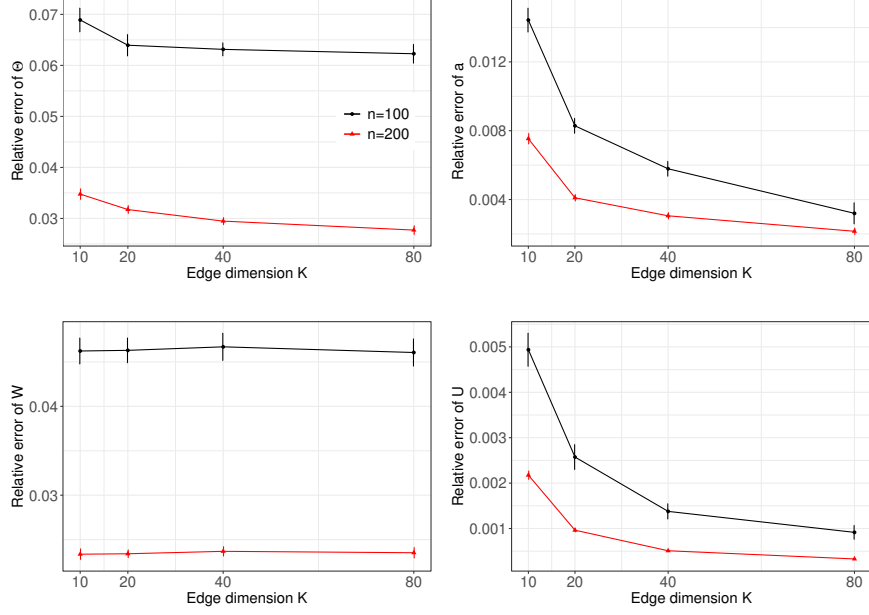


Figure 2: Mean relative errors and their corresponding 95% intervals under varying n and K , while $m = 1$ and edge density at 0.08. The black and red lines mark $n = 100$ and $n = 200$, respectively.

modulate the density of the network; for U^* , we generate its rows u_i^* 's independently from $N_d(0, I)$, which are then scaled to ensure $\|u_i^*\|_2 = 1$ for all i ; for W^* , we randomly select q_0 proportion of its entries to be nonzero and set the rest to zero; values for the nonzero entries are generated independently from Uniform(0.5, 3.5). We set $d = 2$, $m_{ij} = m$, $q_0 = 0.7$ and consider $n = 100, 200$, $K = 10, 20, 40, 80$ and $m = 1, 2, 4, 8$. Also considered are $(a_l, a_u) = (-3.5, -1.8), (-3, -1), (-2, -1), (-1.4, -0.9)$, corresponding to an edge density of approximately 0.04, 0.08, 0.12 and 0.16, respectively.

To evaluate the estimation accuracy, we report relative estimation errors calculated as:

$$\frac{\|\hat{a} - a^*\|_2^2}{\|a^*\|_2^2}, \frac{\|\hat{W} - W^*\|_F^2}{\|W^*\|_F^2}, \min_{R: R^T R = I_k} \frac{\|\hat{U} - U^* R\|_F^2}{\|U^*\|_F^2}, \frac{1}{K} \sum_{k=1}^K \frac{\|\psi(\hat{\Theta}^{(k)}) - \psi(\Theta^{(k)*})\|_F^2}{\|\psi(\Theta^{(k)*})\|_F^2}.$$

where \hat{a} , \hat{W} and \hat{U} are estimators from Algorithm 1, and $\psi(\Theta^{(k)*})$ is true edge probability calculated using a^* , W^* and U^* . Figures 2-3 report the estimation errors of a^* , W^* , U^* and

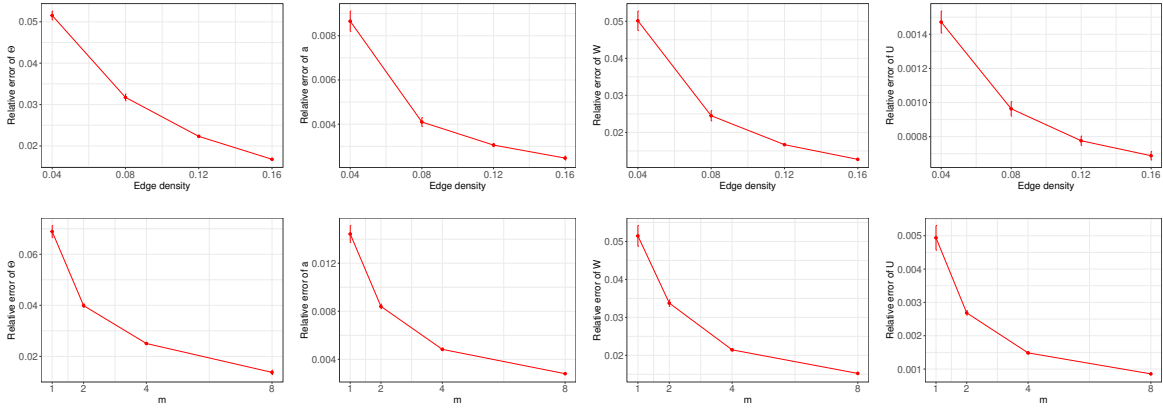


Figure 3: Mean relative errors and their corresponding 95% intervals under varying edge density while $n = 200$, $K = 20$ and $m = 1$ (top panel), and under varying m while $n = 200$, $K = 20$ and edge density at 0.08 (bottom panel).

$\psi(\Theta^{(k)*})$ under various settings, with 95% confidence intervals, over 100 data replications.

It is seen from Figure 2 that estimation errors of a^* and U^* decrease with the network size n and number of layers K , confirming the theoretical results in Theorem 1. The relative estimation error of W^* does not vary with K , as we rescale $\|\hat{W} - W^*\|_F^2$ by $\|W^*\|_F^2$ in calculating the relative error and $\|W^*\|_F^2$ scales with K . Additionally, Figure 3 show that as edge density, modulated by a^* , and the number of edges m increase, the estimation errors of a^* , W^* and U^* decrease.

In Tables 1 and 2, we report the true positive rate (TPR) and false Positive rate (FPR) in estimating the nonzero entries in W^* . The results show that the variable selection accuracy improves with n , m and edge density. The selection accuracy remains relatively stable across different numbers of layers K 's, which is expected since the dimension of W increases with K .

Table 1: True positive rate (TPR) and false positive rate (FPR) in estimating W^* under varying n , K , while $m = 1$ and edge density at 0.08.

	$n = 100$				$n = 200$			
	$K = 10$	$K = 20$	$K = 40$	$K = 80$	$K = 10$	$K = 20$	$K = 40$	$K = 80$
TPR	0.880 (0.045)	0.881 (0.034)	0.883 (0.028)	0.882 (0.023)	0.910 (0.039)	0.925 (0.031)	0.919 (0.024)	0.921 (0.027)
FPR	0.074 (0.039)	0.075 (0.027)	0.076 (0.022)	0.075 (0.024)	0.049 (0.022)	0.068 (0.027)	0.074 (0.028)	0.074 (0.025)

Table 2: True positive rate (TPR) and false positive rate (FPR) in estimating W^* under varying edge density (while fixing $m = 1$) and varying m (while fixing edge density at 0.08), while $n = 200$ and $K = 20$.

	edge density				m			
	0.04	0.08	0.12	0.16	1	2	4	8
TPR	0.850 (0.045)	0.925 (0.031)	0.970 (0.007)	0.986 (0.003)	0.880 (0.045)	0.915 (0.035)	0.948 (0.021)	0.962 (0.019)
FPR	0.128 (0.049)	0.068 (0.027)	0.032 (0.026)	0.015 (0.015)	0.074 (0.039)	0.066 (0.033)	0.058 (0.032)	0.035 (0.029)

6 Analysis of the Enron Email Network

6.1 Data description

The Enron email corpus ([Klimt and Yang, 2004](#)), one of the most extensive publicly available datasets of its kind, contains over 500,000 emails from 158 employees from November 13, 1998 to June 21, 2002. Released by the Federal Energy Regulatory Commission following its investigation of Enron, this dataset provides a unique opportunity to study the communications and organizations within a major corporation during various stages of a financial collapse. The study period can be divided into three stages, as marked by two major events. In February 2001, Enron’s stock reached its peak and then began a dramatic decline following major sell-offs from top executives. It was later found that starting February 2001, concerns about Enron’s accounting practices were increasingly discussed internally. In October 2001, the company’s financial scandal was publicly exposed and the Securities and Exchange Commission began an investigation into Enron’s accounting prac-

Keywords
Enron, corp, gas, power, energy, market, agreement, information, price, deal, contract, credit, legal, fax, review, capacity, phone, north, america, draft, texas, buy, trade, discuss, risk, issue, position, letter, plan, stock, natural, sell, value, customer, pipeline, product, continue, cash, physical, pay, plant, account, picture, attach, earn

Table 3: Extracted keywords sorted by their frequency of occurrences in the corpus.

tices. Accordingly, we consider three stages in our analysis: the pre-decline period from November, 1998, to February, 2001; the decline and pre-bankruptcy period from February, 2001, to October, 2001; and the bankruptcy and post-bankruptcy period from October, 2001, to June, 2002.

Our analysis focused on the emails of 154 employees whose roles and departments are documented in the dataset. These employees are from different departments including gas, legal, transportation, regulatory and government, and wholesale, among others. Data preparation included standard text preprocessing steps such as tokenization, lower-casing, removal of punctuations and stopwords, and stemming. We then employed latent Dirichlet allocation to extract keywords that inform latent topics in the corpus. The 45 extracted keywords are shown in Table 3. To construct the network for each stage, we merged all emails between each pair of nodes into a single document. This process created an undirected network with $n = 154$ nodes and $K = 45$ keywords for each stage, denoted by $\{y_{ij}^{(k)}\}_{i,j \in [154], k \in [45]}$, where $y_{ij}^{(k)} = y_{ji}^{(k)} = 1$ if the merged document between users i and j includes keyword k , and $y_{ij}^{(k)} = y_{ji}^{(k)} = 0$ otherwise. This approach helps to reduce the sparsity of the network and facilitates comparison with other multi-layer network analysis methods. The edge densities of the three networks constructed for stages 1, 2, and 3 are 0.012, 0.010, and 0.009, respectively.

6.2 Alternative approaches and link prediction

We also consider three alternative approaches when analyzing the Enron data:

- **Separate**: This method fits a separate latent space model to each layer, that is, $\Theta^{(k)} = a^{(k)}\mathbf{1}_n^T + \mathbf{1}_n a^{(k)\top} + U^{(k)}U^{(k)\top}$ for $k \in [K]$.
- **Multiness** (MacDonald et al., 2022): This method includes a common latent structure across layers and a separate latent structure for each individual layer, written as $\Theta^{(k)} = VI_{p_0, q_0}V^\top + U^{(k)}I_{p_k, q_k}U^{(k)\top}$ for $k \in [K]$, where $V \in \mathbb{R}^{n \times d_0}$ is the matrix of common latent positions, $U^{(k)} \in \mathbb{R}^{n \times d_k}$ collects the individual latent positions for layer k , and $I_{p, q} = \begin{pmatrix} I_p & 0 \\ 0 & -I_q \end{pmatrix}$.
- **FlexMn** (Zhang et al., 2020): This method considers layer-specific degree heterogeneity a_k , and a common latent position U across layers with a layer-specific scaling matrix $\Lambda^{(k)}$, written as $\Theta^{(k)} = a^{(k)}\mathbf{1}_n^T + \mathbf{1}_n a^{(k)\top} + U\Lambda^{(k)}U^\top$, for $k \in [K]$, where $a^{(k)} \in \mathbb{R}^n$, $U \in \mathbb{R}^{n \times d}$, and $\Lambda^{(k)} \in \mathbb{R}^{d \times d}$.

To compare the performance of above methods in link prediction, we randomly remove 20% entries from each layer and treat them as missing data. We then apply **PLSM**, **Multiness**, **FlexMn**, and **Separate** to the remaining entries and use the fitted model to predict link probabilities for the missing entries. This procedure is repeated 100 times. To ensure a fair comparison, edge cross-validation is used in selecting the latent space dimension for all methods. Figure 4 shows the average precision-recall curves from all four methods. It is seen that **Separate** does not perform well as it cannot borrow information across different layers; **Multiness** might have suffered from over-fitting as there is a large number of sparse layers in each of the three networks. Comparisons of these methods in simulations are included in the Section S7 of supplement.

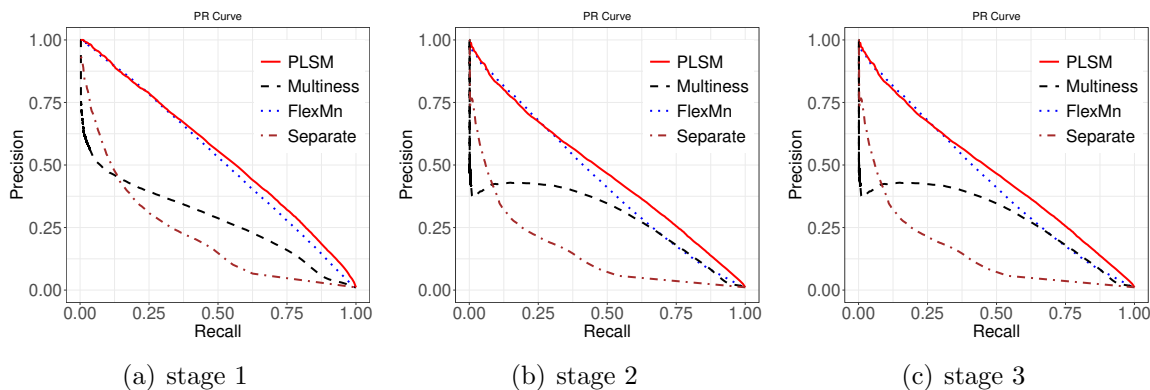


Figure 4: Precision-Recall curves from different methods for out-of-sample link prediction.

6.3 Estimation results from different methods

We apply our proposed method (PLSM) to the three networks from stages 1-3 and use edge cross-validation to select the latent dimension d and the sparsity s . Edge cross validation selected a latent dimension of 10 for stages 1 and 2, and 8 for stage 3. The number of non-zero entries in W was selected as 6653, 6445, and 6237 for stages 1, 2, and 3, respectively. Among the 154 employees, 43 held positions at or above director-level and had significantly more email correspondence. For visualization purposes, we focus on these 43 employees in Figures 5-6. The first row in Figure 5 plots the estimated latent node positions. The estimated latent position u_i 's from PLSM are of unit length, placing them on a K -dimensional sphere. Two nodes with closer latent positions, that is, having a smaller angle between them, are more likely to communicate. The clear clustering pattern of nodes in stages 1 and 2 shows that before bankruptcy, executives in different departments function relatively autonomously. In stage 3, there is a noticeable increase in cross-departmental communications. Also in stage 3, we observe an increase in communications involving the legal department where nodes from the legal department move closer to others, likely due to the legal ramifications of bankruptcy proceedings.

For FlexMn, edge cross-validation selected latent dimensions of 9 for stages 1 and 2, and

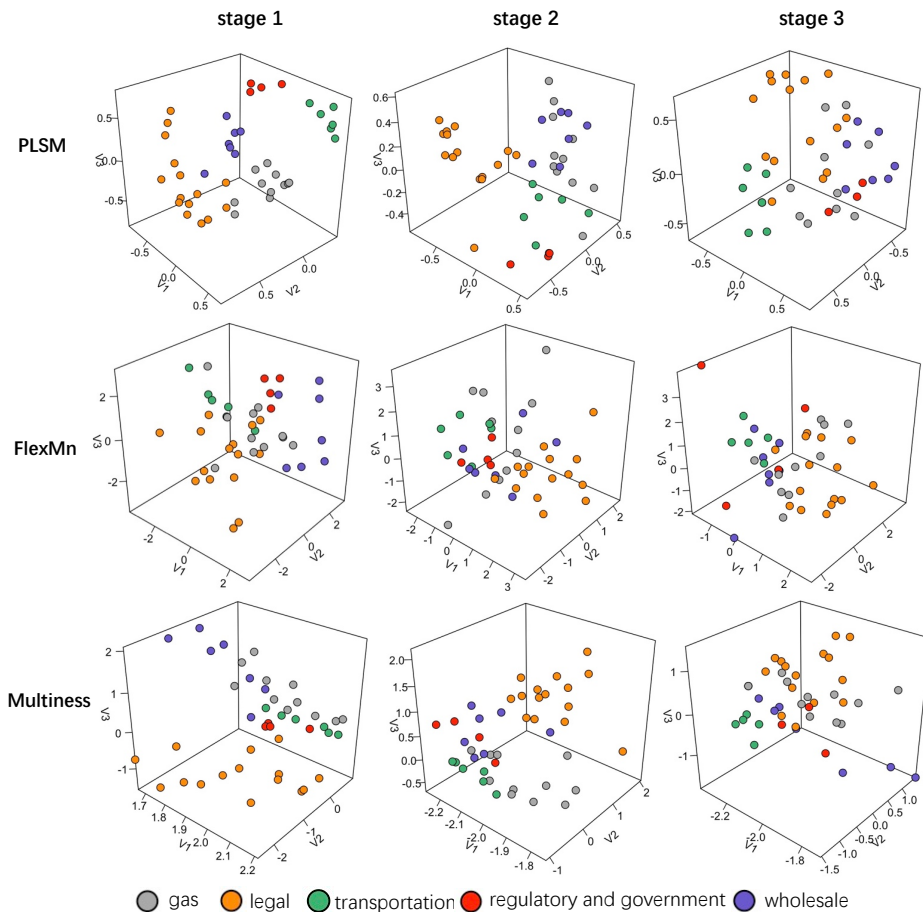


Figure 5: Estimated latent positions by PLSM, FlexMn, and Multiness methods (top to bottom) and stages 1-3 (left to right). For Multiness, only the common latent positions are plotted.

8 for stage 3. For Multiness, edge cross-validation selected 20, the maximum candidate value, for all three stages. The estimated latent positions from FlexMn and Multiness are shown in Figure 5. For Multiness, only the common latent positions are plotted. Multiness displays similar qualitative patterns (up to a rotation) as PLSM in the estimated latent positions. In contrast, FlexMn appears less effective at distinguishing individuals from different departments in stages 1 and 2.

In addition to the unit-length latent positions u_i 's, our proposed method also provides preferential latent positions calculated as $W_{ik}u_i$'s. In particular, the direction of $W_{ik}u_i$ is the same as u_i , while its length $\|W_{ik}u_i\|_2 = W_{ik}$ characterizes the preference or activeness

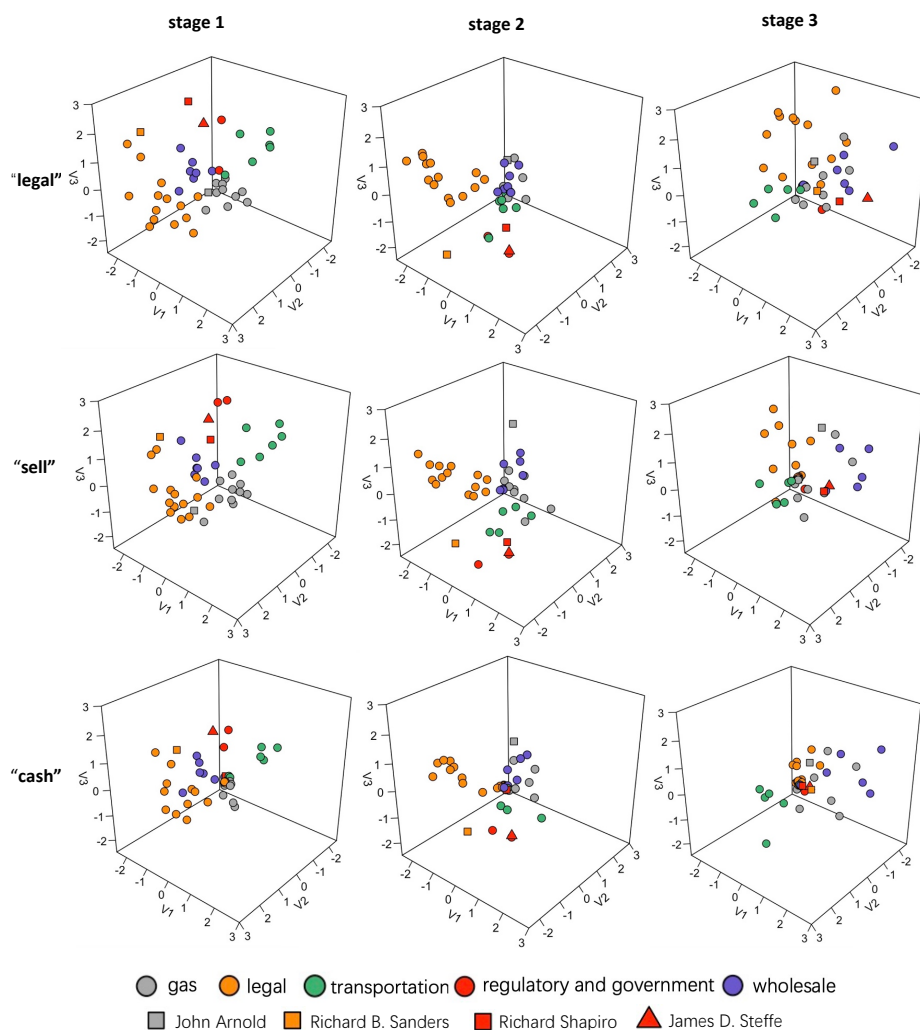


Figure 6: Estimated preferential latent positions $W_{ik}u_i$'s by PLSM on “legal”, “sell”, and “cash”.

of node i on layer k . Figure 6 shows the first three dimensions of $[W_{1k}u_1, \dots, W_{nk}u_n]^\top$ on three keywords: “legal”, “sell”, and “cash.” The keyword “legal” in Enron emails typically pertains to legal advice, agreements and regulatory issues. The keyword “sell” generally involves discussions on asset transactions and marketing strategies. The keyword “cash” often relates to discussions on cash flow management and financial strategies. In stage 1, the legal department is more active in communications involving “legal” compared to “sell” or “cash”. Richard B. Sanders, legal vice president and assistant general counsel, exemplifies this focus. James D. Steffe, vice president of government and part of the regulatory and

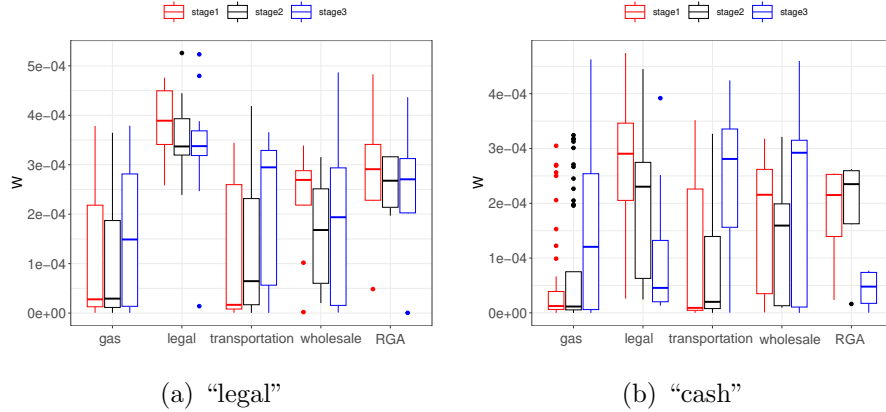


Figure 7: Boxplots of W_{ik} 's for “legal” and “cash” for nodes from different departments. The regulatory and government department is denoted as RGA.

government department, is seen active across all three layers in stage 1. In contrast, Richard Shapiro, vice president of regulatory, shows less engagement in cash-related matters, likely reflecting their differing responsibilities. John Arnold from the gas department shows a significant interest in “sell” and engages more with the legal and wholesale departments in this context. Known as the “king of natural gas”, Arnold played a crucial role in natural gas trading and earned Enron’s largest bonus for his contributions. In stage 2, the gas and wholesale departments move closer compared to stage 1, particularly in discussing legal-related issues. Aside from John Arnold, who remains actively engaged in both “sell” and “cash”, other members of the gas and transportation departments show less activity. In stage 3, the legal department further increases its communication with other departments, especially on cash-related issues. From stages 2 to 3, there is a shift in interests within the regulatory and government department, particularly for individuals such as Richard Shapiro and James D. Steffes. Both moved closer to other departments regarding legal-related matters, likely due to their involvement in post-bankruptcy issues. Additionally, the Legal department’s activity in cash-related discussions decreased.

Figure 7 plots node-layer preferences W_{ik} 's for “legal” and “cash” by departments. It

is seen from Figure 7 (a) that legal, regulatory and government departments are active in legal-related issues across all three stages. Meanwhile, gas and transportation departments had low activity in legal-related issues in stages 1-2, and showed a noticeable increase in their activity in stage 3. Additionally, within the wholesale department, there is an observed increase in the variability of interest levels in legal-related matters from stage 1 to stage 3. Figure 7 (b) shows a noticeable increase in interest regarding cash-related issues in stage 3 from the gas, transportation, and wholesale departments. Following the company’s bankruptcy, communications within these departments frequently include terms such as “cash out” and “cash crunch”. In contrast, the legal and regulatory and government departments show decreased interest in cash-related issues in stage 3.

One attractive feature of our method is that it provides the above insights on node-layer preferences, offering perspectives that are not directly available from other methods.

7 Discussion

Motivated by the enriched text information in network data, the central contribution of this work is a new and flexible preferential latent space model that can offer direct insights on how node-layer preferences modulate edge probabilities. We establish identifiability conditions for the proposed model and tackle model estimation using a computationally efficient algorithm. We further establish the non-asymptotic error bound for the estimator from each step of the algorithm.

Our work can be naturally extended in several directions. One interesting direction is to extend the proposed modeling framework to directed networks. This involves deriving new identifiability conditions and modifying the proposed algorithm. Our work can also be extended to incorporate node-level and/or edge-level covariates. This direction can be

developed following the approach in [Ma et al. \(2020\)](#). We leave these directions to future research.

References

- Agudze, K. M., M. Billio, R. Casarin, and F. Ravazzolo (2022). Markov switching panel with endogenous synchronization effects. *Journal of Econometrics* 230(2), 281–298.
- Arroyo, J., A. Athreya, J. Cape, G. Chen, C. E. Priebe, and J. T. Vogelstein (2021). Inference for multiple heterogeneous networks with a common invariant subspace. *Journal of Machine Learning Research* 22(142), 1–49.
- Athreya, A., D. E. Fishkind, M. Tang, C. E. Priebe, Y. Park, J. T. Vogelstein, K. Levin, V. Lyzinski, Y. Qin, and D. L. Sussman (2018). Statistical inference on random dot product graphs: a survey. *Journal of Machine Learning Research* 18(226), 1–92.
- Bandeira, A. S. and R. van Handel (2016). Sharp nonasymptotic bounds on the norm of random matrices with independent entries. *The Annals of Probability* 44(4), 2479 – 2506.
- Boutin, R., C. Bouveyron, and P. Latouche (2023). Embedded topics in the stochastic block model. *Statistics and Computing* 33(5), 95.
- Bouveyron, C., P. Latouche, and R. Zreik (2018). The stochastic topic block model for the clustering of vertices in networks with textual edges. *Statistics and Computing* 28, 11–31.
- Bramoullé, Y., H. Djebbari, and B. Fortin (2009). Identification of peer effects through social networks. *Journal of Econometrics* 150(1), 41–55.
- Bräuning, F. and S. J. Koopman (2020). The dynamic factor network model with an application to international trade. *Journal of Econometrics* 216(2), 494–515.
- Chen, C. Y.-H., W. K. Härdle, and Y. Klochkov (2022). Sonic: Social network analysis with influencers and communities. *Journal of Econometrics* 228(2), 177–220.
- Corneli, M., C. Bouveyron, P. Latouche, and F. Rossi (2019). The dynamic stochastic topic block model for dynamic networks with textual edges. *Statistics and Computing* 29, 677–695.
- Devlin, J., M.-W. Chang, K. Lee, and K. Toutanova (2018). Bert: Pre-training of deep bidirectional transformers for language understanding. *arXiv preprint arXiv:1810.04805*.
- D’Angelo, S., T. B. Murphy, and M. Alfö (2019). Latent space modelling of multidimensional networks with application to the exchange of votes in eurovision song contest. *The Annals of Applied Statistics* 13(2), 900–930.

- Frank, O. and D. Strauss (1986). Markov graphs. *Journal of the American Statistical Association* 81(395), 832–842.
- Gollini, I. and T. B. Murphy (2016). Joint modeling of multiple network views. *Journal of Computational and Graphical Statistics* 25(1), 246–265.
- Gualdani, C. (2021). An econometric model of network formation with an application to board interlocks between firms. *Journal of Econometrics* 224(2), 345–370.
- Hoff, P. D., A. E. Raftery, and M. S. Handcock (2002). Latent space approaches to social network analysis. *Journal of the American Statistical Association* 97(460), 1090–1098.
- Holland, P. W., K. B. Laskey, and S. Leinhardt (1983). Stochastic blockmodels: First steps. *Social networks* 5(2), 109–137.
- Huang, D., F. Wang, X. Zhu, and H. Wang (2020). Two-mode network autoregressive model for large-scale networks. *Journal of Econometrics* 216(1), 203–219.
- Jin, J., Z. T. Ke, and S. Luo (2024). Mixed membership estimation for social networks. *Journal of Econometrics* 239(2), 105369.
- Jing, B.-Y., T. Li, Z. Lyu, and D. Xia (2021). Community detection on mixture multilayer networks via regularized tensor decomposition. *The Annals of Statistics* 49(6), 3181–3205.
- Joachims, T. (1998). Text categorization with support vector machines: Learning with many relevant features. In *European conference on machine learning*, pp. 137–142. Springer.
- Ke, Z. T., P. Ji, J. Jin, and W. Li (2023). Recent advances in text analysis. *Annual Review of Statistics and Its Application* 11.
- Klimt, B. and Y. Yang (2004). The enron corpus: A new dataset for email classification research. In J.-F. Boulicaut, F. Esposito, F. Giannotti, and D. Pedreschi (Eds.), *Machine Learning: ECML 2004*, Berlin, Heidelberg, pp. 217–226. Springer Berlin Heidelberg.
- Lei, J., K. Chen, and B. Lynch (2020). Consistent community detection in multi-layer network data. *Biometrika* 107(1), 61–73.
- Lei, J. and K. Z. Lin (2023). Bias-adjusted spectral clustering in multi-layer stochastic block models. *Journal of the American Statistical Association* 118(544), 2433–2445.
- Leung, M. P. (2015). Two-step estimation of network-formation models with incomplete information. *Journal of Econometrics* 188(1), 182–195.
- Li, T., E. Levina, and J. Zhu (2020). Network cross-validation by edge sampling. *Biometrika* 107(2), 257–276.
- Lyu, Z., T. Li, and D. Xia (2023). Optimal clustering of discrete mixtures: Binomial, poisson, block models, and multi-layer networks. *arXiv preprint arXiv:2311.15598*.

- Ma, Z., Z. Ma, and H. Yuan (2020). Universal latent space model fitting for large networks with edge covariates. *Journal of Machine Learning Research* 21(1), 86–152.
- MacDonald, P. W., E. Levina, and J. Zhu (2022). Latent space models for multiplex networks with shared structure. *Biometrika* 109(3), 683–706.
- Mihalcea, R. and P. Tarau (2004). Textrank: Bringing order into text. In *Proceedings of the 2004 conference on empirical methods in natural language processing*, pp. 404–411.
- Mikolov, T., K. Chen, G. Corrado, and J. Dean (2013). Efficient estimation of word representations in vector space. *arXiv preprint arXiv:1301.3781*.
- Paul, S. and Y. Chen (2020). Spectral and matrix factorization methods for consistent community detection in multi-layer networks. *The Annals of Statistics* 48, 230–250.
- Pesaran, M. H. and C. F. Yang (2020). Econometric analysis of production networks with dominant units. *Journal of Econometrics* 219(2), 507–541.
- Sachan, M., D. Contractor, T. A. Faruquie, and L. V. Subramaniam (2012). Using content and interactions for discovering communities in social networks. In *Proceedings of the 21st international conference on World Wide Web*, pp. 331–340.
- Salter-Townshend, M. and T. H. McCormick (2017). Latent space models for multiview network data. *The Annals of Applied Statistics* 11(3), 1217.
- Shapiro, A. H., M. Sudhof, and D. J. Wilson (2022). Measuring news sentiment. *Journal of Econometrics* 228(2), 221–243.
- Tropp, J. A. (2012). User-friendly tail bounds for sums of random matrices. *Foundations of computational mathematics* 12, 389–434.
- Wang, F., W. Li, O. H. M. Padilla, Y. Yu, and A. Rinaldo (2023). Multilayer random dot product graphs: Estimation and online change point detection. *arXiv preprint arXiv:2306.15286*.
- Zhang, J. and Y. Chen (2015). Exponential random graph models for networks resilient to targeted attacks. *Statistics and its Interface* 8(3), 267–276.
- Zhang, J., W. W. Sun, and L. Li (2023). Generalized connectivity matrix response regression with applications in brain connectivity studies. *Journal of Computational and Graphical Statistics* 32(1), 252–262.
- Zhang, X., S. Xue, and J. Zhu (2020). A flexible latent space model for multilayer networks. In *International Conference on Machine Learning*, pp. 11288–11297. PMLR.